TU Delft

Delft University of Technology

Document Version
Final published version

Licence
Dutch Copyright Act (Article 25fa)

Citation (APA)
Henzel, J., Bakker, K., Veenstra, S., Isabella, O., Mazzarella, L., Weeber, A., & Theelen, M. (2026). Determining the Reverse Bias Breakdown Voltage of Perovskite Solar Cells. *Solar RRL*, *10*(3), Article e202500875. https://doi.org/10.1002/solr.202500875

Important note
To cite this publication, please use the final published version (if applicable).
Please check the document version above.

Copyright
In case the licence states “Dutch Copyright Act (Article 25fa)”, this publication was made available Green Open Access via the TU Delft Institutional Repository pursuant to Dutch Copyright Act (Article 25fa, the Taverne amendment). This provision does not affect copyright ownership.
Unless copyright is transferred by contract or statute, it remains with the copyright holder.

Sharing and reuse
Other than for strictly personal use, it is not permitted to download, forward or distribute the text or part of it, without the consent of the author(s) and/or copyright holder(s), unless the work is under an open content license such as Creative Commons.

Takedown policy
Please contact us and provide details if you believe this document breaches copyrights.
We will remove access to the work immediately and investigate your claim.

This work is downloaded from Delft University of Technology.

Check for updates

Solar RRL

RESEARCH ARTICLE

Determining the Reverse Bias Breakdown Voltage of Perovskite Solar Cells

Jonathan Henzel[1,2] | Klaas Bakker[1] | Sjoerd Veenstra[1] | Olindo Isabella[2] | Luana Mazzarella[2] | Arthur Weeber[2] | Mirjam Theelen[1]

[1]TNO, Eindhoven, the Netherlands | [2]Photovoltaic Materials and Devices, Delft University of Technology, Delft, the Netherlands

Correspondence: Jonathan Henzel (henzeljonathan@gmail.com) | Mirjam Theelen (mirjam.theelen@tno.nl)

Received: 30 October 2025 | **Revised:** 16 December 2025 | **Accepted:** 17 December 2025

Keywords: degradation | partial shading | perovskite solar cells | reverse bias | stability

ABSTRACT

The degradation of perovskite solar cells due to reverse bias (RB) is one of the remaining challenges hindering the commercialization of the technology. To overcome this challenge, a thorough understanding of and control over the breakdown (BD) voltage are crucial. A prerequisite for this is that the community "speaks the same language," that is, that the reported BD voltages are comparable. A review of literature data shows that the impact of measurement parameters is often unknown and seems to depend strongly on sample properties. It follows that standardization is the only way to reach comparability. Here, a set of measurement parameters to fill this gap is proposed. Additionally, various definitions of a "BD voltage" are used in parallel without any way of relating them to each other; this metric and its determination need to be considered as well. After a thorough discussion of the available definitions, the use of the point of maximum curvature is introduced. Its main advantage is the possible connection to an analytical description of the BD mechanism. In this way, a starting point for scientists new to the field of RB stability is provided, and the ground for a broader discussion in the community is prepared.

1 | Introduction

Concerns about the stability of perovskite solar cells (PSCs) and modules are considered one of the remaining hurdles for the commercialization of this technology [1, 2]. There are various stressors that have been reported to cause degradation in PSCs, for example, light [3, 4], temperature [5], atmosphere [6, 7], and bias [8, 9]. The existing international electrotechnical comission (IEC) standards were designed to test the silicon-based field panels and have been shown to reflect the stability of thin-film photovoltaic (PV) technologies insufficiently [10]. Therefore, the ISOS (International Summit on Organic Photovoltaic Stability) protocols were designed, which define experimental conditions that can be used to investigate the impact of these stressors and combinations of stressors on PSCs in a comparable way [11].

The ISOS-V-1 to ISOS-V-3 protocols deal with electrical bias stability, which includes the degradation caused by reverse biases (RBs) [11]. In a module, RBs can occur when the series-connected cells in a string do not generate the same current. This can be caused by partial shading, when a part of the module area is shaded while the remaining part of the module is illuminated.

A simplified, standardized partial shading event has been described in the work by Dongaonkar [12]: One cell of a module is completely shaded and does not generate any current, while the remaining cells are illuminated. Due to the series connection, this one shaded cell has to pass the current of the current-generating cells. That is only possible when this cell operates at a negative voltage, that is, at a RB.

It has been shown that RB (on cells) and partial shading (on modules) can lead to significant and fast degradation of the power conversion efficiency (PCE) in PSCs [9, 13, 14]. An overview of the mechanisms involved in breakdown (BD) and degradation can be found in the work by Wang et al. [15]. Interestingly, it seems that the degradation rate scales with the RB current and not the RB itself [16, 17]. It follows that—in order to avoid

© 2026 Wiley-VCH GmbH.

degradation in modules—the RB current needs to be limited as much as possible during partial shading events.

Silicon PVs manufacturers employ bypass diodes for this purpose. They are built into modules antiparallel to strings of cells in order to offer a low-resistance current path in case of a RB. However, this solution does not work for modules based on PSCs and other thin-film PV technologies.

One reason is the monolithic interconnection strategy with its long, thin cells that is preferably employed in thin-film PV technologies. That leads to problems with the use of external bypass diodes (for more information, see ref. [18]). Another problem lies in the difference in BD voltage between silicon solar cells and PSCs. The BD voltage (V_{BD}) is a metric that describes the voltage where a RB current flows. A higher V_{BD} means that one bypass diode can protect a "longer" string, so more series-connected cells [13, 18]. A smaller number of bypass diodes per module leads to lower manufacturing costs. Typical BD voltages in crystalline-silicon solar cells are reported to be −15 V [19]. In contrast, often-mentioned values for PSCs are −1 to −5 V [20]. Recently, there have been, however, also reports of higher BD voltages [21–24].

As the BD voltage is a decisive parameter for the RB stability, significant effort has been put into investigating the BD voltage mechanism of PSCs or into manipulating it toward higher ("more negative") voltages [16, 21, 22, 24–26]. However, a well-defined measurement procedure and analysis method—as for the certified PCEs of PSCs—is missing for the BD voltage. Hence, how the BD voltage is measured differs from publication to publication, and information about procedures and parameters applied is often lacking. Additionally, various definitions of the BD voltage and thus methods to analyze the measured data are in use.

As the influence of measurement parameters is generally unknown and the relationships between the different metrics that are called BD voltages are unclear, the published BD voltages cannot be directly compared with each other. That hampers the efforts to find more generally applicable methods of controlling the BD voltage. It also means that we cannot compare different designs and layer stacks.

In this publication, we discuss how to characterize the RB behavior of PSCs. To that end, we take a look at the measurement parameters and conditions playing a role in RB voltage sweeps and their impact on the measurement result. Furthermore, we consider the pros and cons of various BD voltage definitions and demonstrate the superiority of using the point of maximum curvature (PoMC) for that purpose.

2 | How Is the Breakdown Voltage Measured?—Definitions and Implications

In the following, we will use the term "RB BD" for the reversible increase of the current that occurs when a voltage sweep into the RB regime is performed. Here, the current follows an approximately exponential dependence on the voltage and can be described by a tunneling/Zener or, possibly, an avalanche BD mechanism. Its effect on the PCE is a gradual degradation. This BD is depicted in Figure 1a as an RB–*JV* curve with reverse (RV) and forward (FW) sweeps (for details of the measurement procedure, see SI, Table S1). The RV sweep starts in the positive voltage regime and ends in the negative. The FW sweep returns from a negative voltage to the positive voltage regime. To judge the impact on the efficiency, the (standard) *JV* curves from measurements before and after this RB–*JV* sweep are shown as an inset (find measurement details in SI, Table S2). It should be noted that the word "BD" points at the BD of the diode, which is not intrinsically damaging to the solar cell. The solar cell does not necessarily "BD" in the sense of losing its functionality.

This reversible behavior stands in sharp contrast to the "thermal BD" that is depicted in Figure 1b (for measurement details, see SI, Table S1). Here, a sudden, very steep increase of the current to ≈1400 mA cm^{-2} is observed. Its effect on the sample is destructive as it is likely accompanied by the formation of shunts. There might also be a component of thermal runaway where localized heating due to localized current flow leads to a locally-increased conductivity with the two effects escalating toward the destruction of the sample. The inset shows the (standard) *JV* curves

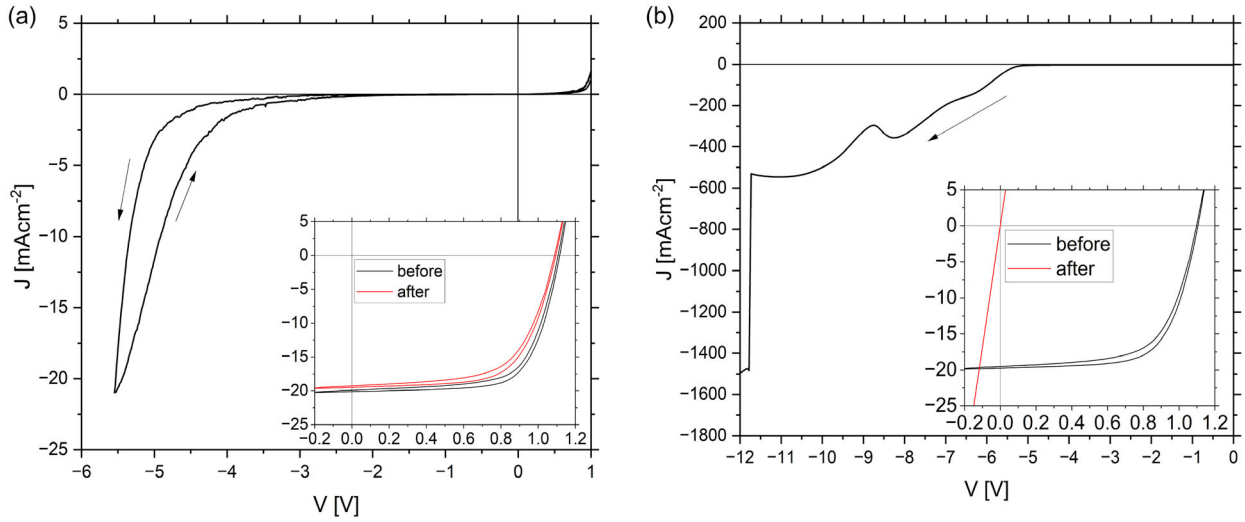


FIGURE 1 | (a) Comparing the reversible "reverse bias breakdown" and (b) the irreversible "thermal breakdown." The insets show standard JV curves from measurements before (black) and after (red) the RB–*JV* measurements. A detailed description of the measurement parameters used for the RB–*JV* measurements can be found in SI, Table S1. The parameters of the *JV* measurements in the insets can be found in SI, Table S2.

2367198x, 2026, 3, Downloaded from https://onlinelibrary.wiley.com/doi/10.1002/solr.202500875 by Tu Delft, Wiley Online Library on [12/02/2026]. See the Terms and Conditions (https://onlinelibrary.wiley.com/terms-and-conditions) on Wiley Online Library for rules of use; OA articles are governed by the applicable Creative Commons License

before and after this RB–*JV* measurement and clearly illustrates the destructive effect of this thermal BD: Shunts dominate the cell behavior and the PCE is reduced to nearly 0% (find measurement details in SI, Table S2).

Furthermore, we will generally talk about absolute BD voltage values. Therefore, a "higher BD voltage (V_{BD})" is one that is more negative. Additionally, we will use the abbreviation "*JV* measurement" for the standard voltage sweep whose purpose it is to measure the PCE of solar cells. When the voltage range is extended to more negative voltages in order to investigate the RB behavior, we will refer to it as "RB–*JV* measurement."

2.1 | Procedures and Parameters in Literature

With these initial definitions out of the way, we can start discussing how the BD voltage is measured. Normally, researchers perform a voltage sweep while measuring the current, similar to the JV measurement that is performed in order to determine the efficiency and other standard solar cell parameters. When it comes to performing an RB–*JV* sweep, there are several measurement parameters to decide on:

- Upper limit (often the starting voltage of the RV sweep)
- Lower limit (either the end voltage of the RV sweep or a current cutoff)
- Scan rate
- Sweep direction (hysteresis measurement)
- External factors: illumination, temperature, and atmosphere

What can we find in literature on PSCs in regard to these parameters? We have summarized the ranges that can be found in literature in Table 1. A table showing the detailed parameters can be found among the data underlying this article (see the Data Availability statement). It should be noted that the values mentioned there are partially assumptions based on the parameters used for standard JV measurements in the same publication or the limits of data that are displayed in graphs.

TABLE 1 | Main measurement parameters of RB–*JV* measurements and the range of values that can be found in PSC literature.

Parameter	Range
Upper limit	0–2 V
Lower limit: Voltage	−0.2 to −20 V
Lower limit: Current density	−1 to −1000 mA cm^{-2}
Scan rate	0.02–10 V s^{-1}
Sweep direction	Mostly only RV; sometimes RV + FW
Illumination	Often unreported; darkness, 0.02–0.25 suns
Temperature	Mostly unreported; −19°C to 45°C
Atmosphere	Mostly unreported; ambient, at controlled relative humidity 35%, in N_2

The extremely wide range used for these parameters is clearly visible and demonstrates why we consider it important to discuss their impact on the measurement result.

2.2 | Literature Survey: Impact of Measurement Parameters

Could these measurement parameters have an impact on the measurement results? Furthermore, are there practical considerations to take into account when deciding on a set of parameters to use? We endeavor to answer these questions in the following sections.

As comparing the RB behavior of PSCs from different publications is difficult, we rely on articles in which the comparison of measurement parameters is attempted. The motivation for these experiments is often increasing the realism of measurements or investigating the BD mechanism. However, a fundamental problem when it comes to determining the impact of measurement parameters on results lies in the limited stability of the PSCs: Any voltage sweep into the RB regime changes the sample, if only temporarily. In a recent publication by Wang et al., the dynamic RB behavior, that is, changes of the RB behavior due to RB–*JV* measurements, is discussed in detail [25]. It is likely that the movement of mobile ions is the origin of this phenomenon. Often, the changes are completely reversible, and the solar cell returns to its original state after some hours of storage in darkness. This still makes the simple comparison of two different measurement settings (e.g., two different voltage scan rates) tedious. Ways around this problem, for example, repeating measurements to estimate the effect of successive voltage sweeps, bring their own problems with them. This might be one of the reasons why information on the impact of some measurement parameters is sparse. Therefore, the quantitative results should be considered with the appropriate care.

2.2.1 | Voltage Scan Rate

The voltage scan rate has been shown to have an impact on the results of standard JV measurements on PSCs. Both the PCE (and thus the other solar cell parameters) and the hysteresis are dependent on the scan rate. The presence of mobile ions is named as one of the origins of this effect [27–29].

According to the widely accepted mechanism of the RB BD in PSCs, mobile ions also play an important role there [9, 30]. Under the influence of the RB, they accumulate at an interface and cause band bending. This facilitates the tunneling of charge carriers into the perovskite and thus the flow of an RB current. Therefore, it stands to reason that the scan rate has an impact on the RB behavior.

The influence of the voltage scan rate has been investigated in several publications:

Bowring et al. compared the RB–*JV* measurements with scan rates of 10 and 0.1 V s^{-1}. They reported that a higher scan rate leads to a higher BD voltage as the mobile ions do not reach steady states faster than the voltage is changed [9]. In their case, the RB–*JV* curve shifted by ≈0.1 V [9]. In contrast, Wang et al. reported a lower BD voltage at higher scan rates, comparing 1, 0.5, and 0.1 V s^{-1} [25]. This contrasting result might be explained by the difference in solar cell layer stack: Wang et al. investigated

2367198x, 2026, 3, Downloaded from https://onlinelibrary.wiley.com/doi/10.1002/solr.202500875 by Tu Delft, Wiley Online Library on [12/02/2026]. See the Terms and Conditions (https://onlinelibrary.wiley.com/terms-and-conditions) on Wiley Online Library for rules of use; OA articles are governed by the applicable Creative Commons License

the behavior of electron transport layer (ETL)-free PSCs, while Bowring et al. used a more traditional p-i-n layout. In Henzel et al., scan rates of 5, 2, 1, 0.5, and 0.1 V s^{-1} were compared. However, it was concluded that the effect of performing several (15) successive measurements (shifting the RB–*JV* curves by about 0.5 V) was interfering with any conclusions regarding the impact of only the scan rate [31].

A more significant impact of the scan rate was reported for the combination of RB and low-intensity illumination by Henzel et al. [31]. There, choosing different scan rates leads to qualitatively different RB–*JV* curves with strongly diverging behavior in the high- and low-RB-current regime. They explained their observations with an activation of mobile ions by the illumination.

Beyond the effect on the measurement result, there is also the effect on the sample itself to consider. PSCs with limited stability might degrade already during RB–*JV* measurements. After all, they are operating in RB during the measurement. As degradation was shown to be a function of RB current and time, a lower scan rate can be expected to lead to more degradation [16].

Some of the available data suggests that the impact of the scan rate on the RB behavior (and therefore a V_{BD}) is small. However, it is doubtful whether any general validity regarding the magnitude of the impact of the scan rate can be claimed. It is likely that this magnitude depends on the properties of the mobile ions (e.g., mobility). These properties, in turn, depend on the perovskite formulation, the macroscopic structure (e.g., grain boundaries as channels for ion migration) [32–34] and other factors. Therefore, the choice of the voltage scan rate should be carefully considered when measuring the V_{BD} via an RB–*JV* measurement.

2.2.2 | Sweep Direction and Hysteresis

The influence of the sweep direction is connected to the issue of RB hysteresis, as this describes a difference between an RV from the FW sweep. As per the definition, the RV sweep starts at a positive voltage and proceeds toward a negative voltage, while the FW sweep starts at a negative voltage and proceeds toward a positive voltage.

The "normal" hysteresis phenomenon in standard *JV* measurements has attracted great interest and research effort since its initial description in 2014 [35]. The general consensus is that the occurrence of hysteresis in *JV* measurements is caused by mobile ions and interface defects [27].

In contrast, the hysteresis phenomenon in RB–*JV* measurements is rarely reported and barely investigated. Specifically, it remains unclear what the "true" BD voltage is and, indeed, whether there is one. Regarding the origin of the RB hysteresis, there is no clarity yet: Assuming that there exist similarities to "normal" hysteresis, it is likely that the same solar cell properties (i.e., mobile ion conductivity and interface defects) play a decisive role. However, to the best of our knowledge, no publication has mentioned any correlation between (standard) hysteresis and RB hysteresis. Another origin of RB hysteresis could involve the storing and discharge of charges (discussed in the work by Henzel et al. [31]). Furthermore, mechanisms that change the BD voltage while the cell is operating in RB on a similar time scale as the voltage sweep could have an impact appearing as hysteresis. However, it should be noted that no detailed research on the origin of RB hysteresis is published.

Wang et al. showed RB–*JV* curves where the difference between RV and FW sweeps amounted to 0.4 V [25]. Henzel et al. also reported both RV and FW sweeps that were showing hysteresis [16]. The difference between the sweeps was most significant in the low-current regime (at RB currents below −5 mA cm^{-2}). The difference between RV and FW sweeps was between 0.2 and 0.7 V [16]. In the work by Aninat et al., RB–*JV* measurements with hysteresis were shown as well. However, they continued their voltage sweep until reaching a current density of −20 mA cm^{-2} and used the voltage there as the BD voltage. Therefore, the issue of hysteresis does not appear in their BD voltages. Finally, Tayagaki et al. measured RB–*JV* hysteresis at low-current densities (≤1 mA cm^{-2}) and at various temperatures [26]. Henzel et al. additionally reported hysteresis in another publication. Again, differences between RV and FW sweeps between 0.2 and 0.7 V were visible [31].

It seems that the effect of the sweep direction on the V_{BD} varies in the few examples where both sweep directions have been reported. The work by Henzel et al. proposes a way of dealing with small differences between RV and FW sweeps. They use the mean of the two BD voltages. The results of both sweep directions should be reported in any case. When hysteresis becomes more significant, however, using a mean might not be a good practice anymore. Then, steady-state measurements, as equivalent to maximum-power-point tracking (MPPT), could be utilized to determine a BD voltage.

2.2.3 | Lower Limit of the Voltage Sweep

In literature, a large variety of lower voltage or current limits are employed (see Table 1). This variety is caused by the different metrics that are supposed to be measured. If $V_{BD} = V$ ($J = -1$ mA cm^{-2}), then it is more than sufficient to use a current density limit of −5 mA cm^{-2}. On the other hand, if $V_{BD} = V$ ($J = J_{SC}$) ≈ V (−20 mA cm^{-2}), then the before-mentioned limit would not be sufficient. Finally, if the desired metric is the voltage where the thermal BD occurs, then even higher current limits and voltages are required.

Can the choice of the lower limit have an impact on the measurement result? Logically speaking, there can be no impact on the initial RV sweep. After all, for the current density at $V = -1$ V in a RV sweep, it does not matter whether the sweep ends at $V = -4$ V or $V = -5$ V. However, the FW sweep and any successive measurements might well be influenced by the choice of the lower limit.

Any effect of the lower limit would be connected to degradation or at least changes to V_{BD} due to operation in RB during the measurement. The idea that operation in RB might affect the RB behavior itself has already been formulated by Bowring et al. [9]. They proposed an electrochemical reaction at an interface that is driven by the RB current. Additional evidence of the effect can be found in the publication of Wang et al., where the effect of successive RB–*JV* measurements is shown in great detail [25]. They argue, however, that the mobile ions accumulating at the interfaces can also lead to an increasing BD voltage.

Therefore, we expect that the RV sweep has an impact on the subsequent FW sweep. The magnitude of this impact is likely dependent on the lower limit since it affects both the RB current and the time spent in RB during the RV sweep. Therefore, the

2367198x, 2026, 3, Downloaded from https://onlinelibrary.wiley.com/doi/10.1002/solr.202500875 by Tu Delft, Wiley Online Library on [12/02/2026]. See the Terms and Conditions (https://onlinelibrary.wiley.com/terms-and-conditions) on Wiley Online Library for rules of use; OA articles are governed by the applicable Creative Commons License

choice of a lower limit should take the stability of the sample into account and which changes to the sample are acceptable.

2.2.4 | Illumination

There are at least two reasons for wanting to add illumination to an experiment on the RB behavior: One is the desire to increase the realism in RB–*JV* measurements and imitate actual operating conditions more closely. Measurements in the dark imitate the simple partial shading event where a cell of a module is completely shaded. Adding illumination tries to extend this scenario to partial shading events where only a part of a cell is shaded or where only a low illumination intensity reaches the cell. A more detailed motivation can be found in Henzel et al. [31]. Another reason could lie in an investigation of the RB BD mechanism itself by disturbing the BD mechanism in a controlled way.

The effect of illumination on the RB behavior has been judged as significant by Wang et al., who found that the BD voltage is strongly reduced by the addition of illumination intensities of about 25 mW cm^{-2} [25]. As an explanation, they proposed that light promotes the generation of mobile ions [25]. In contrast, Jiang et al. reported that the RB behavior and V_{BD} of their PSCs were barely influenced by the addition of 10 mW cm^{-2} [21]. A thorough investigation of the impact of illumination has been published by Henzel et al. [31]. They investigated the effect of different colors of illumination and the effect of illumination in combination with various voltage scan rates. The range of illumination used in their experiments was between 2 and 30 mW cm^{-2}. Finally, they also reported the effect of illumination on steady-state experiments where a fixed current was being injected before illumination was switched on. They found that the light of different wavelengths leads to qualitatively similar results and that the impact of illumination strongly depends on the scan rate. At high scan rates, illumination had a dramatic effect on the V_{BD} values of their cells, while it was insignificant at low scan rates [31]. They proposed an explanation involving the effect of illumination on mobile ions but also an electrochemical reaction that counteracts the effect of the light at low scan rates [31].

Therefore, the effect of illumination might once again depend on the properties and materials of the PSCs. It is clear, however, that the illumination intensity during RB–*JV* measurements should be controlled and reported.

2.2.5 | Temperature

The temperature of the sample can be of interest for two reasons: Firstly, in order to take a further step toward realism and imitate the outdoor situation at increased temperatures [21]. Secondly, as a way to show the dependence on temperature as evidence for the influence of mobile ions that is suggested by the widely accepted BD mechanism [9]. At a scan rate of 0.1 V s^{-1}, the temperature difference between room temperature (RT) and −19°C seemed to cause a difference in $V_{BD} = V$ ($J = -0.5$ mA cm^{-2}) of ≈0.4 V [9]. Jiang et al. did not find a significant difference between the V_{BD} values at RT and 45°C [21]. Tayagaki et al. reported that the RB current increased at lower RBs when the RB–*JV* measurements were performed at higher temperatures. That means that the V_{BD} decreased with increasing temperature, which corroborates the above-mentioned results of Bowring et al. [26]. Both explained this temperature dependence with the effect of temperature on the conductivity of mobile ions. Their conductivity, that is, mobility and/or concentration, influences how they react to external electric fields.

It seems that the temperature can have an influence on V_{BD} via its effect on mobile ions. Thus, the temperature should be taken into account as a measurement parameter.

2.2.6 | Other Parameters

There are two measurement parameters left over that were mentioned in the list at the beginning of this section: One is the upper (voltage) limit of the voltage sweep. To the best of our knowledge, there is no data available on this parameter having an impact on the RB behavior. Xu et al. explained, however, that they pretreated their cells at 0 V for 1 min and then started the RB–*JV* measurements at 0 V with the intention of avoiding "capacitative charging effects" [36]. That implies that starting the voltage sweep at a positive voltage is an inadvertent prebiasing. Unfortunately, we have not seen any data on the effect of positive voltage prebiasing on the RB behavior. Prebiasing with a negative voltage, on the other hand, has been shown to have an effect in the work by Henzel et al. [31]. There, it helped bring the RB behavior of fast voltage sweeps under illumination closer to the behavior of slow voltage sweeps.

The second missing parameter is the atmosphere in which the RB–*JV* measurement is performed. This atmosphere is nearly exclusively "ambient" in the available literature. This could be a problem for two reasons: Firstly, degradation due to ambient atmosphere might occur on a timescale that is similar to the process of performing the RB–*JV* measurements. Secondly, direct interactions between the RB behavior and components of the atmosphere, for example, water, might influence the RB behavior. We are not aware of any publications discussing any of these issues. Therefore, we cannot make a statement about the possible impact they might have. However, it is clear that the parameter "atmosphere" includes information about eventual encapsulation/packaging.

We have seen that a lot is unclear about the impact of measurement parameters and conditions on the resulting V_{BD}. For several parameters, there is some information available. However, even in these cases, the properties of the PSCs are likely to affect the impact of the measurement parameters. That means that there is no "general V_{BD}," there are only BD voltages according to the methods of determining them. That makes it difficult to compare V_{BD} values from different sources.

One solution to that issue is for everyone to use the same measurement parameters. To that end, we will propose two sets of parameters and conditions; one for stable cells and one for less stable cells.

2.3 | Recommendations Toward Standardized Measurements

We have discussed the relevant measurement parameters that impact an RB–*JV* measurement and its results. To that end, we showed the wide range of parameters that has been employed in measurements and experiments regarding the RB behavior of PSCs. Subsequently, we presented data from literature on the impact of these parameters on the measurement results. It seems that the impact often depends on the PSC properties. This makes it difficult to define a general "best practice." Nevertheless, we will propose a set of parameters that can be used as a starting

2367198x, 2026, 3, Downloaded from https://onlinelibrary.wiley.com/doi/10.1002/solr.202500875 by Tu Delft, Wiley Online Library on [12/02/2026]. See the Terms and Conditions (https://onlinelibrary.wiley.com/terms-and-conditions) on Wiley Online Library for rules of use; OA articles are governed by the applicable Creative Commons License

point. Generally, however, reporting the detailed measurement parameters and conditions helps the most.

Two sets of recommended measurement parameters are presented in Table 2. Since literature showed that there is a wide spread in RB stability, we decided to provide recommendations for "stable" and "less stable" samples. Here, "stable" cells are those that do not degrade significantly during one RV–*JV* sweep. This should enable similar experiments on a wider range of PSCs and thus increase inclusivity. A measurement without significant impact on the solar cell quality could also gain entrance into the group of "standard measurements," like *IV* or external quantum efficiency measurements. This would greatly help this field of research.

Our argumentation is the following:

By using an upper limit of 1 V, we incorporate a dark *JV* measurement and therefore information about the state of the solar cell. That way, changes to the cell due to the RB–*JV* measurement are tracked "automatically." Additionally, a certain recovery occurs during the operation in the positive voltage regime at the end of the RB–*JV* measurement.

Using a lower limit of J_{sc} provides information about the whole "realistic" range of operating conditions of a cell in a module. If less impact on the cell is desired, the lower limit can also be limited to $\frac{1}{2}J_{sc}$. That way, the measurement still provides information about the high-RB-current-density regime.

When it comes to the scan rate, a compromise between two opposed considerations has to be found. On the one hand, a lower scan rate means that the cell spends more time operating in RB and therefore experiences more degradation. On the other hand, it has been shown that slow processes occur in PSCs in RB and that it can take a long time to reach an equilibrium upon applying a new bias. A scan rate of $0.2\,V\,s^{-1}$ for stable cells was chosen because it is a typical scan rate for *JV* measurements on PSCs. For less stable cells, using $1\,V\,s^{-1}$ reduces the total charge flowing through the cell and the time spent in RB drastically, and therefore limits degradation.

Hysteresis is a well-known phenomenon in *JV* measurements on PSCs. As the sweep direction can have an impact on the measurement results, it is standard procedure to perform and report both RV and FW sweeps and their respective results. As a hysteresis phenomenon has been shown to occur in RB–*JV* measurements, RV and FW sweeps should also be performed and reported here. The fact that barely anything is known about the RB hysteresis and its connection to "normal" hysteresis increases the importance further.

TABLE 2 | Recommended measurement parameters for the characterization of the reverse bias behavior of PSCs.

Parameter	Recommendation (stable cells)	Recommendation (less stable cells)
Upper limit	1 V	1 V
Lower limit	J_{sc}	$\frac{1}{2}J_{sc}$
Scan rate	0.1 to $0.2\,V\,s^{-1}$	$1\,V\,s^{-1}$
Hysteresis	RV and FW sweep	RV and FW sweep
External conditions	Darkness, RT, ambient atmosphere	Darkness, RT, ambient atmosphere

Finally, when it comes to the external conditions, we decided to keep things simple: RB–*JV* measurements should be performed in complete darkness. This standardized measurement should model the simple and idealized partial shading event of one cell of a module being completely shaded. They can be performed without special temperature control at RT. Regarding the atmosphere, we have not seen any data on an impact of oxygen, humidity, etc. on RB–*JV* measurements. Therefore, as long as the PSCs are stable enough to be characterized in ambient atmosphere via *JV* measurements, we assume that they are not being significantly changed within the time frame of a RB–*JV* measurement.

Despite preconditioning being a relatively common procedure in the perovskite community and in other solar cell technologies, we have decided not to include any such treatment in this list beyond our choice of positive upper limit. The main reason is that it does not seem to be a common procedure to do so in the publications on RB on PSCs. If the impact of an RB–*JV* measurement on the RB behavior causes concern, we recommend performing two RB–*JV* measurements in order to gain an estimation of their effect.

2.4 | Steady-State Measurements

At the end of this section, we would like to comment on a completely different way of determining a BD voltage: measuring the RB behavior in a (quasi) steady state by applying a constant voltage or injecting a constant current. It could be called the functional equivalent of the MPPT. The experiment has been reported in few publications [9, 13, 16, 31]. There, the experiment was not performed to determine a BD voltage and compare it with the BD voltage from a voltage sweep. Instead, the impact of time under RB was the target of these experiments.

One reason for this might be that these cases showed that there does not seem to be a steady state, that is, the voltage or current continues to change in time without stabilizing. In any case, it seems to take some time (several 10 s) to even approximately stabilize when high-current densities are injected. This is shown in the data from the work of Henzel et al. (their ESI, Figure S12) [31]. That means that even if a steady state is reached, significant degradation is to be expected. For these reasons, we do not follow up on this method here.

3 | Defining a Breakdown Voltage

After having discussed how to perform RB–*JV* measurements, we will turn our attention to the following step: How do we get from the raw data of a current (density)–voltage curve to a meaningful metric that describes the RB behavior? In literature, there are various BD voltage definitions available. The problem with that is illustrated in Figure 2a. Different voltages, often describing different parts of the RB–*JV* curve, are all called V_{BD}. One of the reasons for this large variety lies in the different purposes these BD voltages are supposed to fulfill. Three possible purposes are listed in the following:

- Comparability:

The V_{BD} should allow the comparison of PSCs of different batches, with different perovskite formulations, layer stacks, and cell layouts in regard to their RB behavior.

2367198x, 2026, 3, Downloaded from https://onlinelibrary.wiley.com/doi/10.1002/solr.202500875 by Tu Delft, Wiley Online Library on [12/02/2026]. See the Terms and Conditions (https://onlinelibrary.wiley.com/terms-and-conditions) on Wiley Online Library for rules of use; OA articles are governed by the applicable Creative Commons License

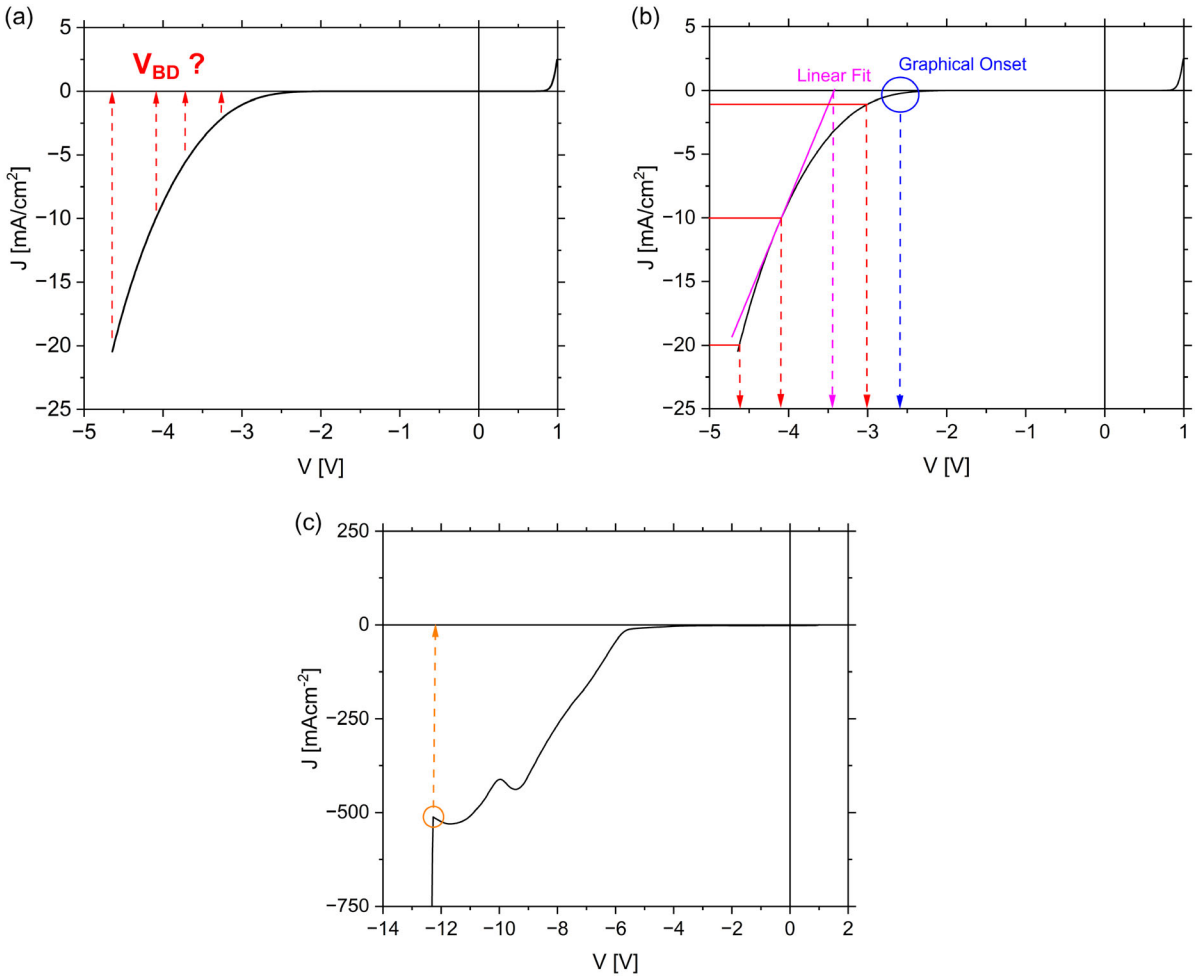


FIGURE 2 | Defining a breakdown voltage. (a) The topic of this section is illustrated: What is the breakdown voltage (V_{BD})? (b) Various definitions of V_{BD} that have been used in publications on PSCs: The onset of the RB current density (blue), three versions of a definition based on fixed current densities (red), and a definition based on a linear fit of the high-RB-current-density regime (magenta). (c) An additional definition based on the sudden current density increase caused by the solar cell shunting.

- Describing real operating conditions:

The V_{BD} should make a statement about the solar cell behavior as part of a module during a realistic partial shading event. Hence, this BD voltage provides information for the design of modules.

- Compatibility with theoretical descriptions:

The V_{BD} should be defined in a way that can be described analytically/mathematically. In that way, a theoretical description of the BD mechanism could be connected to empirical values of V_{BD}.

Additionally, we require that definitions of the BD voltage fulfill some basic requirements: Firstly, the V_{BD} should be clearly, unambiguously defined, so that it describes one voltage (and not a range of voltages) for each sweep direction. Secondly, the V_{BD} should describe the RB behavior and should not be unduly influenced by other factors. We will later see that RB–*JV* curves exist where small or short-lived shunts ("irregularities") affect (only) the low-RB-current-density regime. Since they do not seem to have a significant impact on the high-RB-current-density regime, they should also not dominate the metric describing it.

In the following, we will present the BD voltage definitions that have been used in publications on the RB behavior of PSCs. More definitions can be found when looking at publications about other solar cell technologies, for example, for copper indium gallium diselenide in Puttnins et al. and Szaniawski et al. [37, 38]. Here, we will, however, confine ourselves to those used in the perovskite PV technology and, in the process, propose one additional definition. Furthermore, we will judge the definitions in regard to the above-mentioned purposes and requirements.

3.1 | Definitions in Literature

When categorizing the BD voltage definitions that we will discuss, three groups appear:

- Graphical definitions
  - Graphical onset (see Figure 2b: blue)
  - Thermal BD/shunting (see Figure 2c)
- Fixed current density (see Figure 2b: red)
  - $V\,(J = -1\ \mathrm{mA\ cm^{-2}})$
  - $V\,(J = -10\ \mathrm{mA\ cm^{-2}})$
  - $V\,(J = J_{SC} \approx -20\ \mathrm{mA\ cm^{-2}})$

2367198x, 2026, 3, Downloaded from https://onlinelibrary.wiley.com/doi/10.1002/solr.202500875 by Tu Delft, Wiley Online Library on [12/02/2026]. See the Terms and Conditions (https://onlinelibrary.wiley.com/terms-and-conditions) on Wiley Online Library for rules of use; OA articles are governed by the applicable Creative Commons License

- Advanced analysis techniques
  - * Linear fit (see Figure 2b: magenta)
  - * PoMC

In the following, we will describe them in more detail and discuss their strength and weaknesses.

3.1.1 | Graphical Definitions

Both graphical definitions have in common that the BD voltage is marked by a change in the current density that is visible in a graph.

The definition using the onset of the current density (J) was employed in only one publication [39]. It involves plotting the RB–*JV* curve and then proclaiming the voltage where the current (density) visually increases as V_{BD}. While it is easy to (manually) determine from graphical depictions of RB–*JV* measurement results, it suffers from a serious problem: It is not well-defined. As is shown in Figure 3, the voltage that seems to correspond to the onset of J depends on the graphical depiction. In Figure 3a–c, the same curve is depicted but progressively more "zoomed in." Even though we used axis ranges that ensure that the depicted parts of the curve use most of the graph area (thus, a "realistic" way of presenting the data), V_{BD} seems to shift toward lower voltages. We expect the same to happen when different lower limits (end voltage or current density cutoff) are used for the RB–*JV* measurements. Even when the same axis ranges are used, this "onset" describes rather a voltage range than a specific point on the curve. This vagueness not only causes problems for comparing exact values but also makes it difficult to determine it automatically from RB–*JV* measurement data.

Due to these fundamental issues, it does not seem to be fit for any of the above-mentioned purposes.

The second definition using a graphical depiction was employed by several authors [22–24, 40, 41]. This BD voltage is characterized by a sudden, drastic increase of the current density (see Figure 2c). Based on the assumed mechanism behind this current density increase, it was called "thermal BD (voltage)" in one publication and described as "voltage at which the current spikes suddenly and permanent damage occurs" [41]. We assume this description points at the thermal runaway effect, a feedback loop between localized current flow leading to local Joule heating which increases the local conductivity and therefore leads to increased current flow. It is connected to shunt formation and not to the (Zener or avalanche) diode BD, that is, the reversible RB BD.

As before, a thusly defined BD voltage is easy to determine, not only manually/graphically but also in an automated way. The characteristic current spike can easily be detected by an algorithm. At the same time, its nature as a current spike means that it describes a single point on the RB–*JV* curve and is therefore well-defined. Therefore, it does intrinsically allow the comparison of different solar cells.

It is, however, important to note that current spikes can occur in the low-RB-current regime (i.e., $J \leq -5\,\mathrm{mA\,cm^{-2}}$) without significant effect on the RB behavior at higher current densities (see e.g., Figure 4, red curve with peak). Therefore, an RB–*JV* measurement with a very high lower limit should be used for determining the thermal BD voltage to ensure that the characteristic current spike does lead to the destruction of the solar cell. Since it causes catastrophic damage in the sample, it is a measurement that cannot be reproduced on the same sample and is therefore also not useful as one characterization method among others. Additionally, it also does not allow any statement about the hysteresis, as a damaging RV sweep cannot be followed by an FW sweep.

Furthermore, it is questionable whether the thermal BD voltage is a meaningful metric to describe RB stability: does it indicate an RB threshold with lower RBs being safe for the PSCs? Data from one of the publicationd using this definition answers that question: Even only successive RB–*JV* measurements to $-5\,\mathrm{V}$ performed on samples with thermal V_{BD} values of $-7.6\,\mathrm{V}$ showed complete degradation after a few cycles [41]. Does it describe a realistic degradation mode? In a module without bypass diodes, the largest RB current density that flows through a shaded cell is J_{mpp} if the cell operates beyond its BD. Any voltage with a current density above J_{sc} would therefore be unrealistic. The voltage at which the thermal BD occurs depends, of course, on the solar cell, but in the case depicted in Figure 2c, this spike occurs beyond $-500\,\mathrm{mA\,cm^{-2}}$, so at about $25 \times J_{sc}$.

Finally, as long as the mechanism of the thermal BD is not clear, any connection to the generally accepted RB BD mechanism (tunneling [9]) is not possible. Additionally, if local shunting is the main process leading to thermal BD, the V_{BD} is likely determined by weak spots, for example, particles and other inhomogeneities, and not material or interface properties.

To summarize, while the thermal BD voltage allows for the easy comparison of PSCs, it is not clear whether the underlying cell

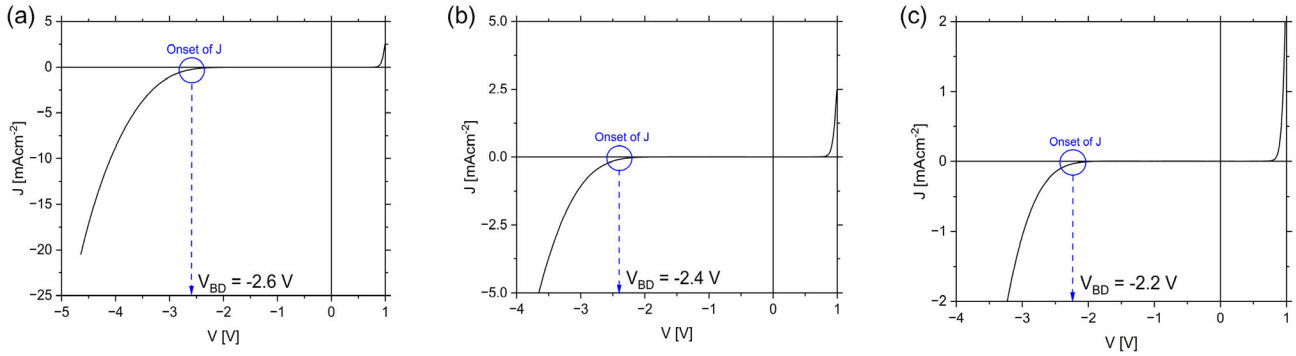


FIGURE 3 | Using the graphical onset of the current density as definition of V_{BD}. The axis ranges shifts from (a–c) which influences the apparent breakdown voltage.

2367198x, 2026, 3, Downloaded from https://onlinelibrary.wiley.com/doi/10.1002/solr.202500875 by Tu Delft, Wiley Online Library on [12/02/2026]. See the Terms and Conditions (https://onlinelibrary.wiley.com/terms-and-conditions) on Wiley Online Library for rules of use; OA articles are governed by the applicable Creative Commons License

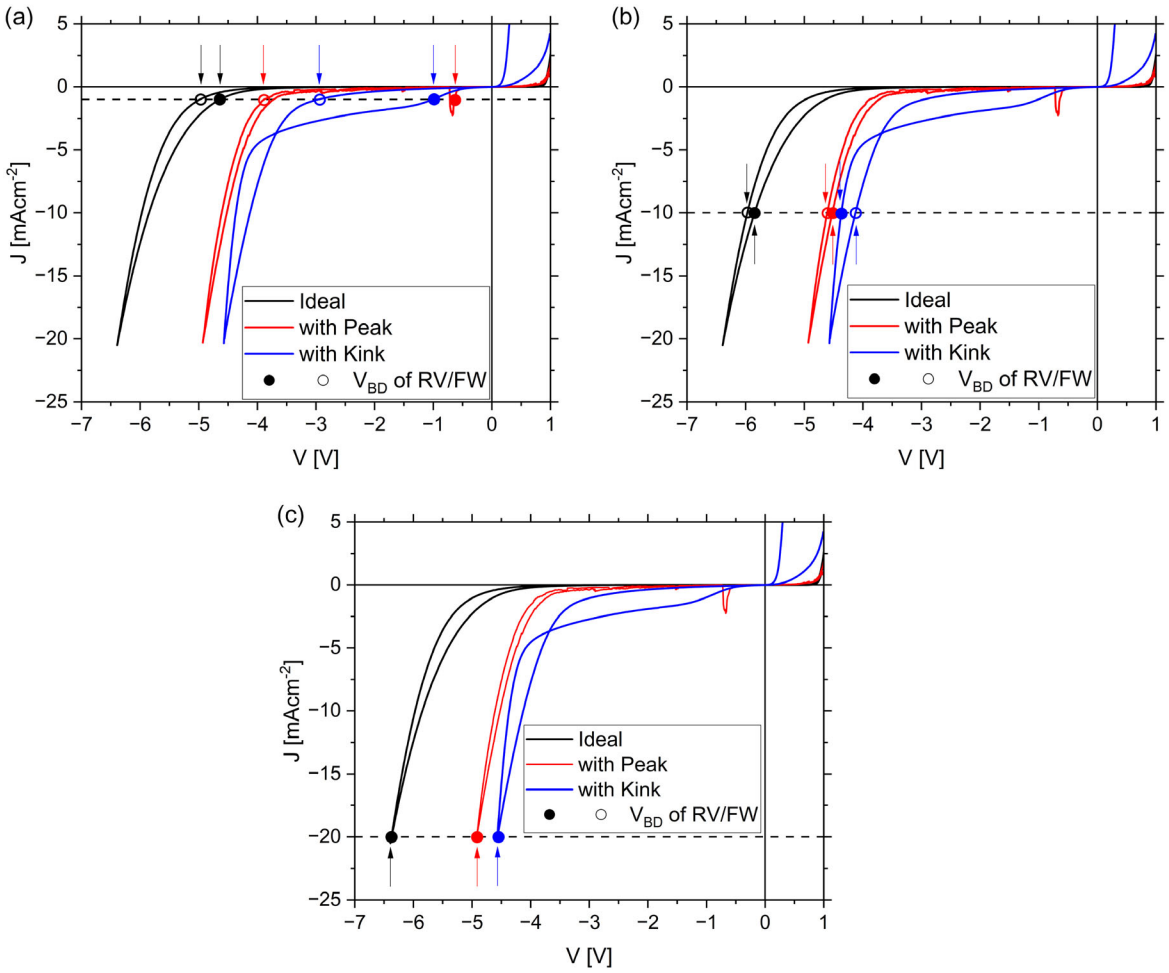


FIGURE 4 | Three breakdown voltage definitions based on fixed current densities ((a) −1 mA cm^{-2}, (b) −10 mA cm^{-2}, (c) −20 mA cm^{-2}) are compared with the aid of three representative RB–*JV* curves (black, red, and blue). The V_{BD} values are marked with circles and arrows. Detailed measurement parameters can be found in SI, Table S3.

property that is compared is decisive for the RB stability. Combined with the practical limitations caused by being a destructive measurement, it does not seem to be a good fit for any of the above-mentioned purposes.

3.1.2 | Fixed Current Density

BD voltage definitions based on a fixed current density are present in various publications. Here, the BD voltage is the voltage where the fixed current density J_{BD} is reached: $V_{BD} = V\,(J = J_{BD})$. The most commonly used version ($J_{BD} = -1\,\text{mA cm}^{-2}$) was proposed by Bowring et al. and subsequently adopted by several other authors [9, 13, 16, 25, 42]. Bowring et al. described their choice of J_{BD} themselves as "arbitrary".

Another publication preferred $J_{BD} = -20\,\text{mA cm}^{-2}$ for being close to J_{SC} and therefore the maximum current that their devices were capable of generating [14]. This current density is the theoretical maximum that a shaded cell would need to pass in a partial shading event on a module without bypass diodes.

Finally, Henzel et al. chose a compromise, using $J_{BD} = -10\,\text{mA cm}^{-2} \approx 0.5\,J_{SC}$ [31]. As their experiments included up to 75 RB–*JV* measurements per cell, they desired to limit degradation and therefore endeavored to decrease the lower limit of their measurements. At the same time, they wanted to prevent their V_{BD} from being influenced too much by the low-RB-current-density regime.

These three versions of this definition are shown in Figure 2b as red, dashed lines and red arrows.

All of them have in common that their corresponding V_{BD} values are very easy to determine, also in an automated way. In principle, these V_{BD} values are also unambiguously defined; at least when the RB–*JV* curve does not show any of the irregularities that are shown in Figure 4: In Figure 4, three RB–*JV* curves are presented. One is close to ideal (black), and one shows a peak before the actual BD, that is, a short-lived, sudden increase of the current density (red). That might be caused by a newly formed or newly activated shunt which heals immediately again. This is a rarely occurring phenomenon with an unclear origin, though we expect a connection to small imperfections in the solar cell area. The last curve shows a pre-BD, that is, an irregular early BD that leads to a significant RB current even before the actual, exponential BD occurs (blue curve in Figure 4). This phenomenon was caused by the addition of blue, low-intensity illumination on RB–*JV* measurements with low scan rates (e.g., 0.1 V s^{-1}). The data shown here stems from the publication by Henzel et al. [31]. We use these RB–*JV* curves to demonstrate how BD voltage definitions based

2367198x, 2026, 3, Downloaded from https://onlinelibrary.wiley.com/doi/10.1002/solr.202500875 by Tu Delft, Wiley Online Library on [12/02/2026]. See the Terms and Conditions (https://onlinelibrary.wiley.com/terms-and-conditions) on Wiley Online Library for rules of use; OA articles are governed by the applicable Creative Commons License

on fixed current densities deal with ideal and nonideal RB–*JV* results.

In Figure 4a, the three RB–*JV* curves are shown with the addition of a horizontal line that marks $J_{BD} = -1\ mA\ cm^{-2}$. Filled circles and empty circles mark the BD voltages of the RV sweep and FW sweep, respectively. For the ideal RB–*JV* curve, the two V_{BD} values also convey information about the RB hysteresis. For the RB–*JV* curve with the peak, one red circle marks the peak since it crosses J_{BD}, while the empty circle is placed at the actual V_{BD} values of the RV and FW sweeps. The blue circles mark very different V_{BD} values; one is dominated by the pre-BD, the other by the "real" BD.

Thus, we have seen that using $J_{BD} = -1\ mA\ cm^{-2}$ does work well for ideal RB–*JV* curves. However, whenever there are irregularities present that affect the low-RB-current regime, they can significantly influence the determined V_{BD} values. As can be seen in the same graph, the same irregularities do not significantly impact the high-RB-current regime. Additionally, the irregularities are not present at all in the FW sweep. That calls into question whether the V_{BD} values that use $J_{BD} = -1\ mA\ cm^{-2}$ represent the RB behavior accurately.

When we take a look at Figure 4b,c, we see how the definitions using $J_{BD} = -10\ mA\ cm^{-2}$ and $J_{BD} = -20\ mA\ cm^{-2}$ fare with the same RB–*JV* curves. Their advantage of not being unduly influenced by the RB behavior in the low-RB-current behavior is clearly visible.

In return, while determining these V_{BD} values at $0.5J_{sc}$ and J_{sc}, (irreversible) degradation is likelier to occur. Jiang et al. found that their PSCs experienced irreversible degradation when passing J_{mpp} (which is still lower than J_{sc}). Cells that had to pass lower current densities ($\leq -1\ mA\ cm^{-2}$) showed irreversible or reversible degradation [21]. That fits with the conclusion of Henzel et al. that degradation is current-driven [16]. In the light of these observations, using $J_{BD} = -10\ mA\ cm^{-2}$ seems to be a compromise that enables measuring V_{BD} without degrading the samples while still conserving the meaning of the metric as representing the high-RB-current regime. This approach suffices for comparing cells, at least.

To summarize, all the definitions using a fixed current density possess the advantage of easy determination. However, $J_{BD} = -1\ mA\ cm^{-2}$ and $J_{BD} = -10\ mA\ cm^{-2}$ are completely arbitrary values. Therefore, the V_{BD} values determined using them as fixed current densities do not have any meaning in the sense of describing the state of operation or physics. Only $V_{BD} = V\,(J = J_{SC})$ stands out, as it can be connected to the worst-case scenario in a module without bypass diodes. Finally, using a high J_{BD} as a fixed current density negates the impact of irregularities in the low-RB-current regime on the metric. On the other hand, the deleterious effects of RB–*JV* measurements (degradation to destruction) increase with a higher lower limit.

3.1.3 | A Linear Fit

Another publication proposed a BD voltage definition that requires a slightly more advanced analysis procedure [21]. They performed a linear fitting in the current density range of -5 to $-15\ mA\ cm^{-2}$. The V_{BD} is then the voltage where the linear fit function crosses the *x*-axis. The intention behind that procedure was generating V_{BD} values for the two types of RB–*JV* curves they observed: Most showed a gradual increase of the RB current with increasing RB, but some showed a sudden increase.

We imitated that analysis procedure, using a script that performs a linear fit on the RB–*JV* curve in the above-mentioned current density range. We executed this procedure on the same three representative RB–*JV* curves that we introduced in Figure 4. The results of this analysis are shown in Figure 5. The measurement results are always split into RV sweep (black) and FW sweep (red). The linear fit functions corresponding to RV and FW sweeps are plotted in the same graph as black and red dashed lines, respectively, with the corresponding V_{BD} values marked by black and red dots.

In Figure 5a,b, we can see that the described approach of the linear fit works well with ideal curves and curves with a peak in the low-RB-current-density regime since this method only uses the data beyond $-5\ mA\ cm^{-2}$. It is, therefore, not influenced by irregularities in the low-RB-current regime.

Only when the irregularities have an impact on the curve within the fitting region does the resulting quality of the fit decrease and not mirror the high-RB-current regime as well. This is visible in Figure 5c where the pre-BD behavior has a significant impact on the RV sweep at current densities up to $-10\ mA\ cm^{-2}$. To improve this, the fitting region would have to be restricted to a regime of higher current densities. Therefore, this definition is generally able to deliver a V_{BD} that can be used to compare solar cells.

However, while ignoring differences in BD mechanisms with possibly very different consequences for the cells might be helpful for a quantitative investigation, it might be disadvantageous as long as the BD mechanisms are not understood in detail. Additionally, the V_{BD} resulting from this definition is an arbitrary number that does not have a technical or physical meaning and lacks an analytical description. So, it might be useful for comparison but does not allow any further conclusions. Finally, in order to use the whole current density range (-5 to $-15\ mA\ cm^{-2}$, as proposed by the authors) and include information about hysteresis, a voltage sweep to at least $-20\ mA\ cm^{-2}$ seems to be necessary, with all the disadvantageous effects previously mentioned.

With that, we have discussed the various definitions of the BD voltage that have been previously used to describe the RB behavior of PSCs. Our basic requirements included being well-defined and not unduly influenced by the behavior in the low-RB-current regime. These needs were met by a few definitions: Those based on a fixed current density of -10 and $-20\ mA\ cm^{-2}$ and the linear fit method.

Of these, only one is not just an arbitrary number and therefore useful for more than only comparison: The definition of the fixed current density of $-20\ mA\ cm^{-2}$ can be connected to a partial shading scenario of a module without bypass diodes.

3.2 | Proposing an Additional Definition

After having presented all the BD voltage definitions present in literature on PSCs, we would like to propose an additional definition. In 1971, Mahadevan et al. published a list with definitions that had been used to describe the RB BD of semiconductor p–n junctions [43]. One of the entries is annotated with the assessment: "tedious though capable of analytical formulation and of universal applicability." Especially the aspect of the analytical formulation has attracted our interest since that implies the possibility of connecting the V_{BD} to theoretical descriptions of the BD mechanism. This property is notably missing among the

2367198x, 2026, 3, Downloaded from https://onlinelibrary.wiley.com/doi/10.1002/solr.202500875 by Tu Delft, Wiley Online Library on [12/02/2026]. See the Terms and Conditions (https://onlinelibrary.wiley.com/terms-and-conditions) on Wiley Online Library for rules of use; OA articles are governed by the applicable Creative Commons License

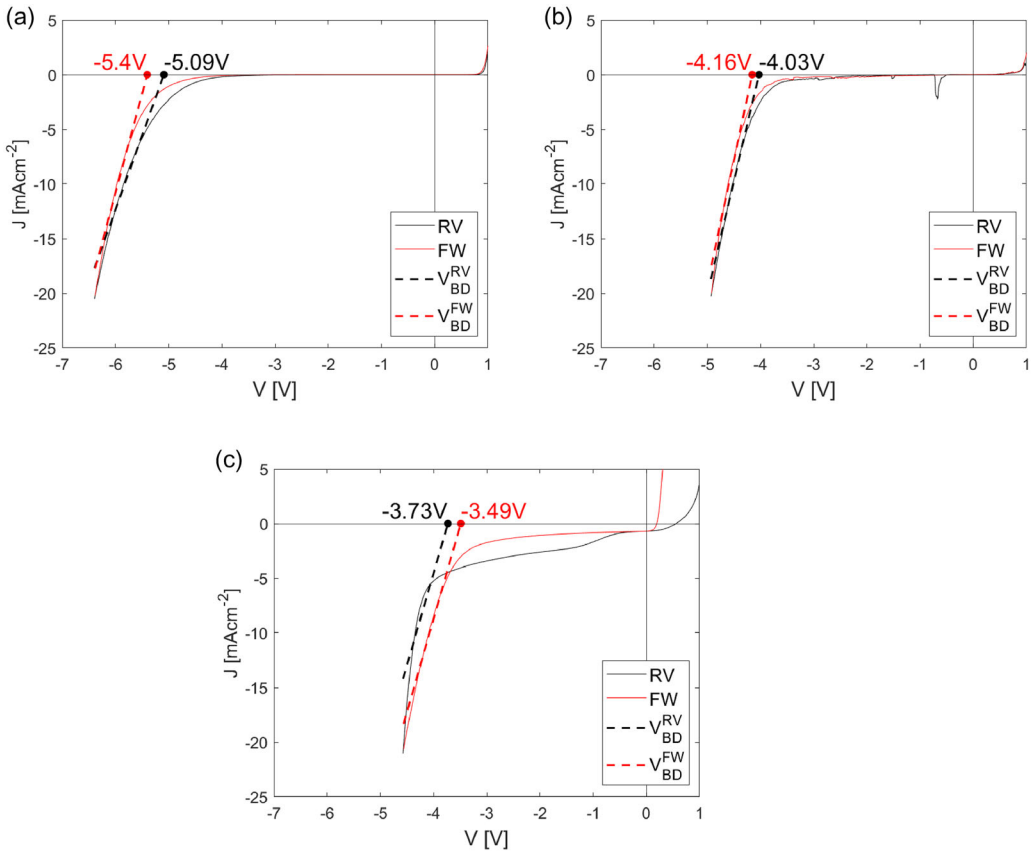


FIGURE 5 | The linear fit method proposed in ref. [21] is executed on three representative RB–*JV* curves ((a) ideal, (b) with peak, (c) with pre-breakdown) to test the impact of the low-RB-current-density regime. The resulting V_{BD} values are marked with circles.

previously described definitions. The criterion, that is, the definition, that is described here, is the PoMC in the RB–*JV* curve.

While the PoMC is, in principle, well- and unambiguously-defined, the practical execution of its determination leaves room for variance. Therefore, we will add some additional constraints to our definition:

- Definition of the curvature κ
- Method of derivation
- Fit function

We use the following definition of the curvature [44]:

$$\kappa = \frac{|\ddot{J}|}{\left(1+\dot{J}^2\right)^{\frac{3}{2}}} \tag{1}$$

with J being the current density, $\dot{J}$ its first derivative with respect to the voltage, and $\ddot{J}$ its second derivative with respect to the voltage.

Regarding the method of derivation, there are two different options. One is to perform numerical differentiations. This option suffers from two disadvantages: The previously shown irregularities would disturb the numerical differentiations. The peak shown in Figure 4, would lead to massive, local curvatures. Additionally, even slight nonideal behavior of the RB–*JV* curve makes the use of a smoothing algorithm necessary. This introduces additional variance to the result and complexity to the procedure.

The second option is to perform curve fitting on the data to approach it with a function and then calculate the derivatives and the PoMC of this fit function. This stands and falls with the quality of the fit, that is, how well the analytical expression mirrors the measured RB–*JV* data. We have not found an expression with a physical background (e.g., describing Fowler–Nordheim tunneling) that has been confirmed to describe the results of our RB–*JV* measurements well. As developing a physical model is beyond the scope of this publication, we choose a purely empirical approach. For the sake of keeping this procedure simple, we will use a simplified relationship between current density (J) and applied bias (V): We choose a single-term exponential function with only empirical coefficients a, b, c:

$$J = a \cdot e^{b \cdot V} + c \tag{2}$$

This function can describe most of our RB–*JV* curves reasonably well (see SI, Figure S1). However, our interest lies in determining a PoMC as accurately as possible. Therefore, we use a two-step process to increase the accuracy of the fit around the expected PoMC. This method of restricting the data range used for fitting seems to be the most generally applicable.

1. Fit of complete RB–*JV* curve ($V \leq 0$V)
2. Calculation of PoMC (intermediate)
3. Fit of data around PoMC (final)
4. Calculation of PoMC (final)

2367198x, 2026, 3, Downloaded from https://onlinelibrary.wiley.com/doi/10.1002/solr.202500875 by Tu Delft, Wiley Online Library on [12/02/2026]. See the Terms and Conditions (https://onlinelibrary.wiley.com/terms-and-conditions) on Wiley Online Library for rules of use; OA articles are governed by the applicable Creative Commons License

More details of the procedure can be found in the Supporting Information (Note S1).

The result of this procedure is shown in Figure 6. There, the RV and FW sweeps of RB–*JV* measurements are displayed as black and red solid lines, respectively. The fit functions are plotted within their range as blue and magenta dashed lines, respectively. Blue and magenta symbols mark the resulting PoMC. Again, we are using three RB–*JV* curves as examples. One is ideal (Figure 6a), one shows a peak (Figure 6b), and the third shows the pre-BD behavior in the RV sweep (Figure 6c). We see that, for the ideal curve (a) and the curve with a peak (b), the fit functions follow the data very well in the assigned data ranges. The BD voltage values of the RV and FW sweeps also reflect the hysteresis in the corresponding data well. When it comes to the curve with a kink (c), the FW sweep is described very well, too. However, the RV sweep with the significant kink carries this method in its present state to its limit. Nonetheless, it is still possible to extract a V_{BD}-value.

Here, it is necessary to mention that the PoMC is not the "knee" of an exponential curve. In fact, what is described as "knee" is an illusion of the linear plotting, depends on the choice of axes, and is not related to a special point of the curve [45]. This statement is demonstrated in the SI, Figure S2 where we plot the same exponential function with very different axes and see that the "knee" appears at wildly different values of x. In contrast, the PoMC describes a unique point of the curve that is well-defined and which is not dependent on the axes of the graph.

Thus, we have successfully extracted the PoMC for use as BD voltages from the three example RB–*JV* measurements. This

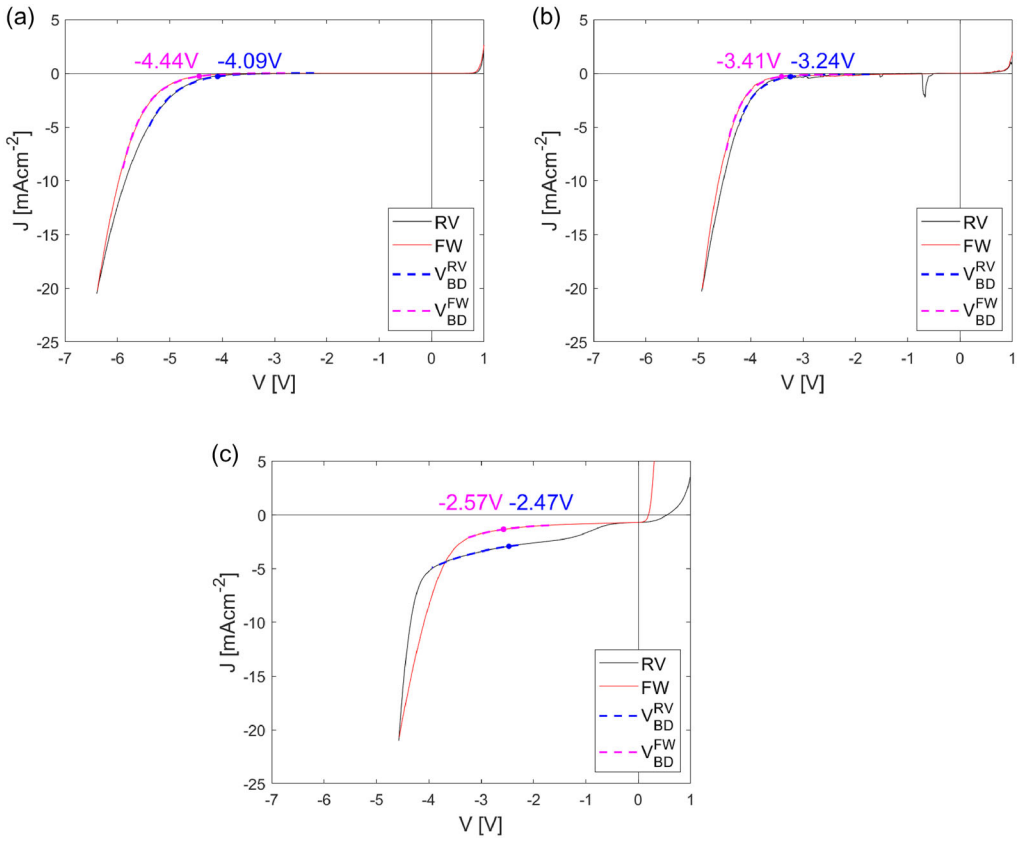


FIGURE 6 | The newly proposed definition using the power of maximum curvature is tested on the three representative RB–*JV* curves. The resulting V_{BD} values are marked by circles.

TABLE 3 | The V_{BD} values of the three representative RB–*JV* measurements, as determined by the various different definitions.

V_{BD}-Definition	Ideal (RV/FW), V	w. Peak (RV/FW), V	w. Illumination (RV/FW), V
Fixed J: $J_{BD} = -1$ mA cm^{-2}	−4.63/−4.98	−0.63/−3.88	−1.00/−2.93
Fixed J: $J_{BD} = -10$ mA cm^{-2}	−5.83/−5.98	−4.51/−4.60	−4.35/−4.11
Fixed J: $J_{BD} = -20$ mA cm^{-2}	−6.37/−6.37	−4.91/−4.91	−4.56/−4.56
Linear fit	−5.09/−5.40	−4.03/−4.16	−3.49/−3.73
PoMC	−4.09/−4.44	−3.24/−3.41	−2.47/−2.57

2367198x, 2026, 3, Downloaded from https://onlinelibrary.wiley.com/doi/10.1002/solr.202500875 by Tu Delft, Wiley Online Library on [12/02/2026]. See the Terms and Conditions (https://onlinelibrary.wiley.com/terms-and-conditions) on Wiley Online Library for rules of use; OA articles are governed by the applicable Creative Commons License

V_{BD} has the unique advantage of being analytically expressible, so that it can be potentially connected to a theoretical description of the BD mechanism. Due to fitting a function to it, this method is also mostly independent of possible irregularities in the low-RB-current regime.

Also, the demand of comparability is fulfilled since this method of analyzing RB–*JV* curves should result in very similar V_{BD} values as long as the quality of the fit is acceptable. Thus, even using different fit functions should not lead to very different BD voltages. Nonetheless, it surely is good practice to report the detailed procedure, if not the whole analysis script.

There are, however, also downsides to this definition of the BD voltage: First, this V_{BD} does not have a meaning that is intuitively accessible. It can be analytically expressed, but the voltage is not related to a specific operating point of the solar cell. Second, the analysis is comparatively complex which, could serve as a hurdle for users. Finally, there is one area where the most important improvement can be made: Extending or modifying the fit in connection with an accompanying physical model could allow more detailed investigations into the parameters influencing the RB BD of PSCs. However, especially for the case of illumination (shown in Figure 6c), developing a well-fitting model that allows for quantitative predictions is challenging [31].

TABLE 4 | Measurement parameters used during the RB–*JV* measurements whose results are shown in Figure 7.

Parameter	Data of Figure 7
Upper limit	1 V
Lower limit: Current density	J_{sc}
Scan rate	1 V s^{-1}
Hysteresis	RV and FW sweep
External conditions	Darkness, RT, ambient atmosphere
Additional note	Second RB–*JV* measurement

3.3 | Comparing the Breakdown Voltages

After having discussed various ways of measuring and determining the BD voltage, we will demonstrate the impact of using different BD voltage definitions. To that end, we will first compare the V_{BD} values of the three representative RB–*JV* curves that result from the different described definitions. These V_{BD} values are listed in Table 3.

Furthermore, we compare the results of RB–*JV* measurements performed on a batch of semitransparent, p-i-n PSCs. Details of the fabrication of the PSCs can be found in the Supporting Information (Note S2). The detailed measurement parameters are shown in Table 4. We largely followed the recommendations for less stable cells but used a lower limit of J_{sc} to make the comparison with BD voltages of the fixed current densities possible. Additionally, we performed two RB–*JV* measurements on each

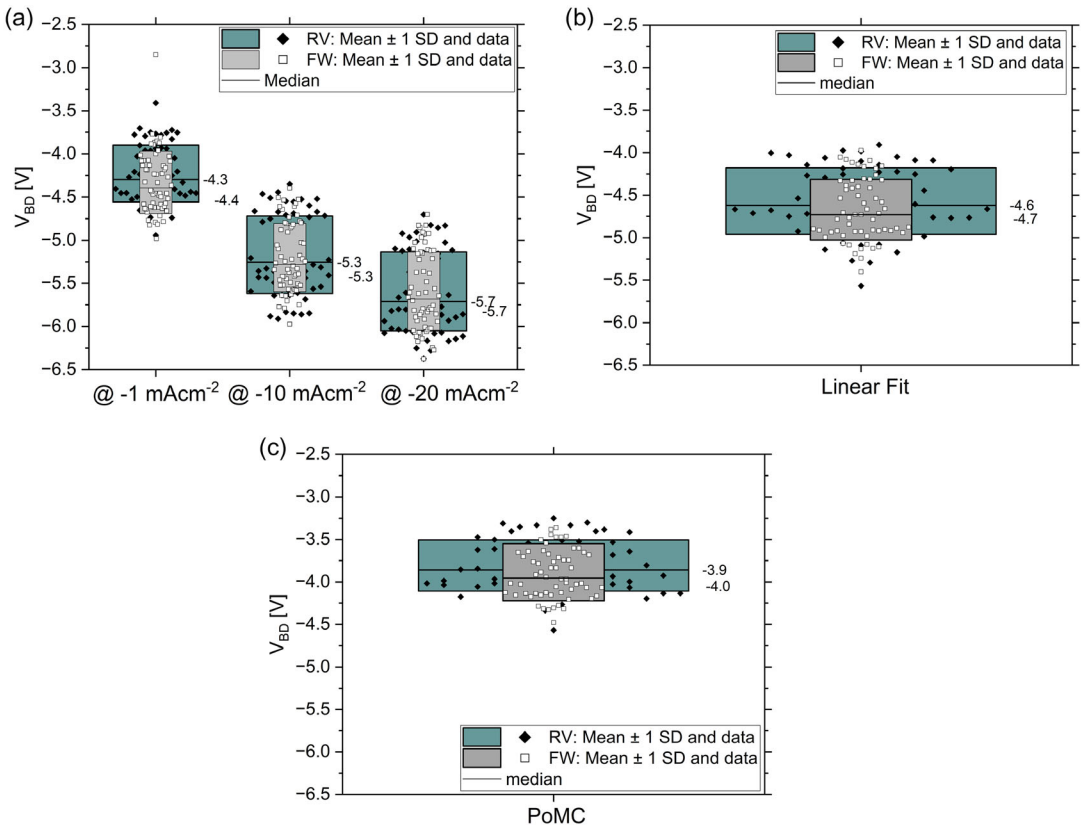


FIGURE 7 | The breakdown voltages of a batch of 60 PSCs, determined using five different definitions, are compared: (a) three versions based on fixed current densities, (b) the linear fit method from the work from ref. [21], and (c) the method using the PoMC. The detailed measurement parameters are listed in Table 4.

2367198x, 2026, 3, Downloaded from https://onlinelibrary.wiley.com/doi/10.1002/solr.202500875 by Tu Delft, Wiley Online Library on [12/02/2026]. See the Terms and Conditions (https://onlinelibrary.wiley.com/terms-and-conditions) on Wiley Online Library for rules of use; OA articles are governed by the applicable Creative Commons License

cell to estimate the effect of the measurement itself. The data shown here is from the second measurement.

In Figure 7, the BD voltages of a batch of 60 PSCs are displayed. In Figure 7a, the three definitions based on fixed current densities are shown; in Figure 7b, the V_{BD} values of the linear fit method; and in Figure 7c, the corresponding result using the PoMC. The black diamonds mark the data points determined from RV sweeps, while the white squares come from the FW sweeps. The green box shows the standard deviation (SD) around the mean of the values from the RV sweeps, and the gray boxes the corresponding information for the FW sweeps. The horizontal lines with attached labels mark the medians. The distribution of the data points on the *x*-axis does not have a meaning in any of the box plots of Figure 7.

We observe how the BD voltage definitions compare when the analysis is performed on many RB–*JV* curves. The medians of the V_{BD} values of the RV sweeps vary between −5.7 and −3.9 V. The SD differs slightly between 0.3 V for the PoMC method to 0.5 V for the fixed current density method using $J_{BD} = -20\,\mathrm{mA\,cm^{-2}}$. In the SI, Figure S3, we show example data points and how they change between the definitions.

With that, we have shown the significant differences in the magnitude of V_{BD} that can be caused by using different definitions. At the same time, it seems that the SD of the RB behavior is relatively independent of the analysis method. This serves as validation for the proposed V_{BD} definition and proof that it can be used to describe the RB behavior of PSCs as long as a reversible BD occurs. This should be valid for all PSC variants, so not only p-i-n layer stacks but also n-i-p as long as the immediate formations of shunts can be prevented.

4 | Conclusions

The information at which voltage PSCs break down and pass current in RB is of utmost importance for both the research on the BD mechanism and for dealing with the underlying issue of partial shading. However, standards for characterizing PSCs in regard to their RB behavior are missing.

This study showed how measurement parameters and conditions vary among publications on the topic. At the same time, data on the impact of measurement parameters on the result are sparse, with sometimes contrary observations reported. A significant dependence on sample-specific properties is presumed. Additionally, the method of defining and determining the BD voltage also varies wildly in available literature, without any information about the relationship between different BD voltage definitions available.

That suggests that standardization is the only way to comparability. To that end, we proposed detailed sets of measurement parameters and conditions that can serve as a starting point for newcomers to the field and as input for a discussion in the community. Additionally, a new definition of the BD voltage is proposed: Using the PoMC provides a comparable BD voltage that can be analytically expressed. Therefore, it can prospectively be connected to theoretical descriptions of the BD voltage mechanism.

That touches on one important gap in our understanding of the RB behavior of PSCs: A detailed formulation of the BD mechanism that incorporates the unique properties of perovskites would be of great help to refine both the measurement procedure and the method of determining a BD voltage.

Acknowledgments

The authors acknowledge Johannes Lambooij and Corné Frijters (both TNO) for their part in the fabrication of samples. This work was funded through governmental funding via the Kennis Investerings Project (KIP) Solar and the Early Research Program (ERP) STAR of TNO financed by the Ministry of Climate Policy and Green Growth and Ministry of Economic Affairs.

Funding

This study was supported by Ministry of Climate Policy and Green Growth and Ministry of Economic Affairs.

Conflicts of Interest

The authors declare no conflicts of interest.

Data Availability Statement

Data for this article are available at 4TU. ResearchData under https://doi.org/10.4121/1a649ecf-3165-47a9-b794-3f02ff42cc80.

References

1. D. Lan and M. A. Green, "Combatting Temperature and Reverse-Bias Challenges Facing Perovskite Solar Cells," *Joule* 6, no. 8 (2022): 1782.

2. Y. Rong, Y. Hu, A. Mei, et al., "Challenges for Commercializing Perovskite Solar Cells," *Science* 361, no. 6408 (2018): eaat8235.

3. F. Lang, O. Shargaieva, V. V. Brus, H. C. Neitzert, J. Rappich, and N. H. Nickel, "Influence of Radiation on the Properties and the Stability of Hybrid Perovskites," *Advanced Materials* 30, no. 3 (2018): 1702905.

4. S. W. Lee, S. Kim, S. Bae, et al., "UV Degradation and Recovery of Perovskite Solar Cells," *Scientific Reports* 6 (2016): 38150.

5. J. A. Schwenzer, L. Rakocevic, R. Gehlhaar, et al., "Temperature Variation-Induced Performance Decline of Perovskite Solar Cells," *ACS Applied Materials and Interfaces* 10, no. 19 (2018): 16390.

6. J. Yang, B. D. Siempelkamp, D. Liu, and T. L. Kelly, "Investigation of CH3NH3PbI3 Degradation Rates and Mechanisms in Controlled Humidity Environments Using In Situ Techniques," *ACS Nano* 9, no. 2 (2015): 1955.

7. D. Bryant, N. Aristidou, S. Pont, et al., "Light and Oxygen Induced Degradation Limits the Operational Stability of Methylammonium Lead Triiodide Perovskite Solar Cells," *Energy and Environmental Science* 9, no. 5 (2016): 1655.

8. M. V. Khenkin, K. M. Anoop, E. A. Katz, and I. Visoly-Fisher, "Bias-Dependent Degradation of Various Solar Cells: Lessons for Stability of Perovskite Photovoltaics," *Energy and Environmental Science* 12, no. 2 (2019): 550.

9. A. R. Bowring, L. Bertoluzzi, B. C. O'Regan, and M. D. McGehee, "Reverse Bias Behavior of Halide Perovskite Solar Cells," *Advanced Energy Materials* 8, no. 8 (2018): 1702365.

10. K. Domanski, E. A. Alharbi, A. Hagfeldt, M. Grätzel, and W. Tress, "Systematic Investigation of the Impact of Operation Conditions on the Degradation Behaviour of Perovskite Solar Cells," *Nature Energy* 3, no. 1 (2018): 61.

11. M. V. Khenkin, E. A. Katz, A. Abate, et al., "Consensus Statement for Stability Assessment and Reporting for Perovskite Photovoltaics based on ISOS Procedures," *Nature Energy* 5, no. 1 (2020): 35.

2367198x, 2026, 3, Downloaded from https://onlinelibrary.wiley.com/doi/10.1002/solr.202500875 by Tu Delft, Wiley Online Library on [12/02/2026]. See the Terms and Conditions (https://onlinelibrary.wiley.com/terms-and-conditions) on Wiley Online Library for rules of use; OA articles are governed by the applicable Creative Commons License

12. S. Dongaonkar, C. Deline, and M. A. Alam, "Performance and Reliability Implications of Two-Dimensional Shading in Monolithic Thin-Film Photovoltaic Modules," *IEEE Journal of Photovoltaics* 3, no. 4 (2013): 1367.

13. R. A. Z. Razera, D. A. Jacobs, F. Fu, et al., "Instability of P–I–N Perovskite Solar Cells under Reverse Bias," *Journal of Materials Chemistry A* 8, no. 1 (2020): 242.

14. R. Aninat, K. Bakker, J. Henzel, et al., "Mapping the Partial Shading Degradation in a Monolithically Integrated Perovskite Module," *Progress in Photovoltaics: Research and Applications* 34, no. 1 (2025): 60.

15. C. Wang, L. Huang, Y. Zhou, et al., "Perovskite Solar Cells in the Shadow: Understanding the Mechanism of Reverse-Bias Behavior toward Suppressed Reverse-Bias Breakdown and Reverse-Bias Induced Degradation," *Advanced Energy Materials* 13, no. 9 (2023): 2203596.

16. J. Henzel, K. Bakker, M. Najafi, et al., "Impact of the Current on Reverse Bias Degradation of Perovskite Solar Cells," *ACS Applied Energy Materials* 6, no. 22 (2023): 11429.

17. L. J. Geerligs, M. Najafi, N. J. Bakker, et al., in *Tandem PV Workshop* (2022).

18. E. J. Wolf, I. E. Gould, L. B. Bliss, J. J. Berry, and M. D. McGehee, "Designing Modules to Prevent Reverse Bias Degradation in Perovskite Solar Cells when Partial Shading Occurs," *Solar RRL* 6, no. 3 (2022): 2100239.

19. B. B. Pannebakker, A. C. de Waal, and W. G. van Sark, "Photovoltaics in the Shade: One Bypass Diode Per Solar Cell Revisited: Photovoltaics in the Shade," *Progress in Photovoltaics: Research and Applications* 25, no. 10 (2017): 836.

20. D. Di Girolamo, O. Dupré, G. Giuliano, et al., "Silicon/Perovskite Tandem Solar Cells with Reverse Bias Stability down to −40 V. Unveiling the Role of Electrical and Optical Design," *Advanced Science* 11, no. 31 (2024): 2401175.

21. F. Jiang, Y. Shi, T. R. Rana, et al., "Improved Reverse Bias Stability in P–I–N Perovskite Solar Cells with Optimized Hole Transport Materials and Less Reactive Electrodes," *Nature Energy* 9, no. 10 (2024): 1275.

22. X. Ren, J. Wang, Y. Lin, et al., "Mobile Iodides Capture for Highly Photolysis- and Reverse-Bias-Stable Perovskite Solar Cells," *Nature Materials* 23, no. 6 (2024): 810.

23. J. Wang, G. Nie, W. Huang, et al., "Reconstruction and Solidification of Dion–Jacobson Perovskite Top and Buried Interfaces for Efficient and Stable Solar Cells," *Nano Letters* 24, no. 38 (2024): 11873.

24. N. Li, Z. Shi, C. Fei, et al., "Barrier Reinforcement for Enhanced Perovskite Solar Cell Stability under Reverse Bias," *Nature Energy* 9, no. 10 (2024): 1264.

25. C. Wang, L. Huang, Y. Guo, et al., "Abnormal Dynamic Reverse Bias Behavior and Variable Reverse Breakdown Voltage of ETL-free Perovskite Solar Cells," *Solar RRL* 7, no. 20 (2023): 2300456.

26. T. Tayagaki, H. Kobayashi, K. Yamamoto, T. N. Murakami, and M. Yoshita, "Effects of Partial Shading and Temperature-Dependent Reverse Bias Behaviour on Degradation in Perovskite Photovoltaic Modules," *Solar Energy Materials and Solar Cells* 279 (2025): 113229.

27. D. A. Jacobs, Y. Wu, H. Shen, et al., "Hysteresis Phenomena in Perovskite Solar Cells: The Many and Varied Effects of Ionic Accumulation," *Physical Chemistry Chemical Physics* 19, no. 4 (2017): 3094.

28. J. Thiesbrummel, S. Shah, E. Gutierrez-partida, et al., "Ion-Induced Field Screening as a Dominant Factor in Perovskite Solar Cell Operational Stability," *Nature Energy* 9, no. 6 (2024): 664.

29. V. M. Le Corre, J. Diekmann, F. Peña-Camargo, et al., "Quantification of Efficiency Losses Due to Mobile Ions in Perovskite Solar Cells via Fast Hysteresis Measurements," *Solar RRL* 6, no. 4 (2022): 2100772.

30. L. Bertoluzzi, J. B. Patel, K. A. Bush, et al., "Incorporating Electrochemical Halide Oxidation into Drift-Diffusion Models to Explain Performance Losses in Perovskite Solar Cells under Prolonged Reverse Bias," *Advanced Energy Materials* 11, no. 10 (2021): 2002614.

31. J. Henzel, K. Bakker, S. Veenstra, et al., "The Impact of Low-Intensity Illumination on the Reverse Bias Behavior of Perovskite Solar Cells," *Journal of Materials Chemistry A* 13, no. 37 (2025): 31755.

32. Y. Ma, Y. Cheng, X. Xu, et al., "Suppressing Ion Migration across Perovskite Grain Boundaries by Polymer Additives," *Advanced Functional Materials* 31, no. 3 (2021): 2006802.

33. Y. Shao, Y. Fang, T. Li, et al., "Grain Boundary Dominated Ion Migration in Polycrystalline Organic–Inorganic Halide Perovskite Films," *Energy and Environmental Science* 9, no. 5 (2016): 1752.

34. J. S. Yun, J. Seidel, J. Kim, et al., "Critical Role of Grain Boundaries for Ion Migration in Formamidinium and Methylammonium Lead Halide Perovskite Solar Cells," *Advanced Energy Materials* 6, no. 13 (2016): 1600330.

35. H. J. Snaith, A. Abate, J. M. Ball, et al., "Anomalous Hysteresis in Perovskite Solar Cells," *Journal of Physical Chemistry Letters* 5, no. 9 (2014): 1511.

36. Z. Xu, H. Bristow, M. Babics, et al., "Reverse-Bias Resilience of Monolithic Perovskite/Silicon Tandem Solar Cells," *Joule* 7, no. 9 (2023): 1992.

37. S. Puttnins, S. Jander, A. Wehrmann, et al., "Breakdown Characteristics of Flexible Cu(In,Ga)Se2 Solar Cells," *Solar Energy Materials and Solar Cells* 120 (2014): 506.

38. P. Szaniawski, P. Zabierowski, J. Olsson, U. Zimmermann, and M. Edoff, "Advancing the Understanding of Reverse Breakdown in $Cu(In,Ga)Se_2$ Solar Cells," *IEEE Journal of Photovoltaics* 7, no. 4 (2017): 1136.

39. D. Bogachuk, K. Saddedine, D. Martineau, et al., "Perovskite Photovoltaic Devices with Carbon-Based Electrodes Withstanding Reverse-Bias Voltages up to –9 V and Surpassing IEC 61215:2016 International Standard," *Solar RRL* 6, no. 3 (2021): 2100527.

40. N. Liu, Q. Zou, Y. Li, et al., "Halogen Bonding Enable Improved Performance and Stability of Dion–Jacobson Perovskite Solar Cells," *Angewandte Chemie, International Edition* 64, no. 27 (2025): e202500131.

41. L. Lanzetta, L. Huerta Hernandez, B. Vishal, et al., "Tin–Lead Perovskite Solar Cells with Enhanced Reverse Bias Stability," *ACS Energy Letters* 10, no. 5 (2025): 2093.

42. I. E. Gould, C. Xiao, J. B. Patel, and M. D. McGehee, in *2021 IEEE 48th Photovoltaic Specialists Conference (PVSC)*, (2021): 1365.

43. S. Mahadevan, S. M. Hardas, and G. Suryan, "Electrical Breakdown in Semiconductors," *Physica Status Solidi A* 8, no. 2 (1971): 335.

44. R. G. Mortimer, *Mathematics for Physical Chemistry* (Elsevier Inc., 2005).

45. G. Pu, "*The Inflection Point of the Exponential Function*," 2024, https://georgerpu.github.io/blog/2024/exp-inflection-point/.

Supporting Information

Additional supporting information can be found online in the Supporting Information section. **Supporting Fig. S1:** A RB-JV measurement and the results of fitting the data with exponential functions. The intermediate PoMC values resulting from these fit functions are marked. **Supporting Fig. S2:** One exponential function displayed in graphs with different axes. **Supporting Fig. S3:** The breakdown voltages of a batch of 60 PSCs, determined using five different definitions are compared: a) Three version based on fixed current densities, b) the linear fit method, and c) the method using the PoMC. The VBD-values of three cells are colored in red, green and blue in all three sub-figures. The detailed measure ment parameters are listed in the main text in Table 4. **Supporting Table S1:** Measurement parameters used during the RB-JV measurements whose results are shown Figure 1 in the main text.

2367198x, 2026, 3, Downloaded from https://onlinelibrary.wiley.com/doi/10.1002/solr.202500875 by Tu Delft, Wiley Online Library on [12/02/2026]. See the Terms and Conditions (https://onlinelibrary.wiley.com/terms-and-conditions) on Wiley Online Library for rules of use; OA articles are governed by the applicable Creative Commons License

Supporting Table S2: Measurement parameters used during the (standard) JV measurements whose results are shown Figure 1 (in sets) in the main text. **Supporting Table S3:** Measurement parameters used during the RB-JV measurements whose results are shown Figure 4, 5, and 6 in the main text.

2367198x, 2026, 3, Downloaded from https://onlinelibrary.wiley.com/doi/10.1002/solr.202500875 by Tu Delft, Wiley Online Library on [12/02/2026]. See the Terms and Conditions (https://onlinelibrary.wiley.com/terms-and-conditions) on Wiley Online Library for rules of use; OA articles are governed by the applicable Creative Commons License